

PSEUDO REACTION RATE IN THE AC RESPONSE OF AN ELECTROLYTIC CELL

J. ROSS MACDONALD and CARMIE A. HULL

Department of Physics and Astronomy, University of North Carolina, Chapel Hill, NC 27514 (U.S.A.)

(Received 29th August 1983)

ABSTRACT

When theoretical impedance–frequency “data” calculated from an exact small-signal ac solution of the transport equations for an unsupported intrinsic-conduction situation are fitted to an appropriate equivalent circuit using nonlinear complex least squares, one finds that a non-zero apparent charge transfer resistance is necessary for a good fit even when charges of one sign are taken completely blocked at the electrodes and those of opposite sign are taken as completely unblocked. Normally, one would expect no reaction resistance under these conditions. This effect only occurs when positive and negative charges have different mobilities and may be ascribed to ambipolar drag of one set of charges on the other set. Here we demonstrate the effect and derive approximate relations to be used in data analysis which should allow an accurate estimate of the true reaction rate to be obtained when it is not too large. The practical limit to the maximum reaction rate which can be derived from experimental impedance data for the present situation is shown to depend on both a diffusion coefficient and the Debye length.

INTRODUCTION

We consider here the small-signal ac response of a system comprised of two identical plane parallel metallic electrodes separated by a distance l and containing material with a dielectric constant ϵ , taken frequency independent over the range of frequencies of interest. It is assumed that the material between the electrodes contains mobile uni–univalent positive and negative charges, with mobilities at the temperature of measurement of μ_p and μ_n , respectively. Thus we are concerned with an unsupported situation applying to either solid or liquid electrolytes. We assume that the mobile charges arise from the dissociation of neutral centers (e.g. a salt in liquids; the basic material in aliovalent single crystals, yielding Schottky or Frenkel defects; or even electrons and holes in electronic semiconductors). We thus consider an unbiased intrinsic conduction situation and further assume that dissociated pairs recombine bimolecularly [1,2].

The exact small-signal solution of the above problem, with [in fact] extrinsic as well as intrinsic conduction and generation–recombination, has been given but is very complicated in the general case [1]. Here we initially consider the often encountered situation where charges of one sign, say the positive ones, are com-

pletely blocked at the electrode, and the negative ones are completely unblocked, show ohmic behavior, and may thus be considered to react at the electrodes exceedingly rapidly (infinite reaction rate, k_n). With the signs reversed this is a common parent-ion electrode situation for ionic conductions. (Although the sign choice is arbitrary, we use the present selection of signs and reaction rates for agreement with previously published work embodying this selection.)

Let the electrode reaction rates for positive and negative charge carriers be denoted k_p and k_n , where here we shall always choose $k_p = 0$ and will initially take $k_n = \infty$. Let us normalize all rates so that $\rho_j \equiv (l/2)(k_j/D_j)$, where D_j is the diffusion coefficient of the j th type of charges. Thus $\rho_n \equiv (l/2)(k_n/D_n)$. Next, denote the mobility ratio as $\pi_m \equiv \mu_n/\mu_p$. Clearly as $\mu_n \rightarrow \infty$, since there is no blocking assumed for negative carriers, the impedance of the system must approach zero for all frequencies, an uninteresting condition. We are interested here in the opposite situation, that where $\mu_n \leq \mu_p$ and π_m becomes small.

We need to define a few more parameters. Let the geometrical capacitance of the system be denoted by $C_1 \equiv \epsilon/4\pi l$, where all extensive quantities will be given for unit electrode area. Further, let the high-frequency limiting resistance be denoted $R_1 \equiv [(ec_0/l)(\mu_p + \mu_n)]^{-1}$, where c_0 is the common undisturbed bulk value of the concentration of the positive and negative charge carriers. Then the dielectric relaxation time τ_D is just $R_1 C_1$. Next, we need the quantities Λ and ξ , where Λ is a measure of the intrinsic dissociation ratio (small when $\Lambda \ll 1$ and approaching full dissociation for $\Lambda \gg 1$); and $\xi \equiv \tau_1/\tau_D$, where τ_1 is the intrinsic recombination relaxation time [1]. We shall be entirely concerned with $\xi \gg 1$, so we are not dealing with relaxation semiconductor behavior [3]. Finally, define $M \equiv l/2L_D$, the number of two-mobile Debye lengths in half of the cell. Here $L_D \equiv [\epsilon kT/8\pi e^2 c_0]^{1/2}$, where k is Boltzmann's constant, T is the thermodynamic temperature, and e is the proton charge.

For increased generality, it is useful to deal with normalized quantities. Let us therefore normalize all resistances and impedances with R_1 and all capacitances with C_1 ; then $R_N \equiv R/R_1$, $C_N \equiv C/C_1$ and the normalized frequency is $\Omega \equiv \omega\tau_D \equiv \omega R_1 C_1$. For most experimental impedance measurements, even at the maximum measured frequency, $\Omega < 1$.

The system and conduction situation described above is a common one yet it has not been fully analyzed so far even though its exact solution exists [1]. Usually, impedance or admittance data are compared with the predictions of a plausible equivalent circuit by graphical or least squares methods [4–6] in order to determine values of the equivalent circuit parameters. Although it is very desirable to interpret these first-level parameters in terms of more basic and microscopic material/electrode characterizing parameters [1,7,8], this is not always done. As we shall show, in the present situation there is an appreciable chance, for fast electrode reactions, that the most natural microscopic interpretation will be erroneous, leading to an incorrect estimate of k_n unless the present analysis is employed.

As discussed elsewhere in detail [5], we believe that the most objective way to obtain equivalent circuit parameter estimates from experimental impedance or

admittance data is to use nonlinear complex least squares fitting (NCLSF), usually with weighting based on uncertainties taken proportional to data value magnitudes (W1 weighting). But given a specific mathematical-model impedance function solution, as we have in the present intrinsic conduction situation, there are two ways of proceeding. First and most appropriate, the model (which may not be well approximated by any simple equivalent circuit) may be fitted directly with NCLSF to obtain estimates of all the basic microscopic parameters immediately. When the model is as complicated as it is even in the present intrinsic situation, this is a substantial undertaking. Nevertheless, we plan to add this model to our powerful NCLSF program and invite those with appropriate data to either send them to us for such analysis or request a tape of the full program, which will be provided on a cost basis.

Alternatively, one can fit to an equivalent circuit if there is reason to prefer a specific one and use the resulting circuit element estimates to solve for microscopic parameter values when an appropriate model is available. This procedure will usually be less accurate than that above and may introduce some bias in basic parameters estimates. Here we shall reverse this procedure in order to find an equivalent circuit appropriate for the intrinsic conduction situation and to find approximate connecting equations leading from circuit parameter values to microscopic ones. Thus, we start with specific choices of the basic model parameters, here R_1 , C_1 , π_m , M , ρ_p , ρ_n , Λ , and ξ , and generate theoretical impedance "data" from the model. These data are then fitted to a given circuit using NCLSF. By carrying out this procedure for several different circuits, we have found one which is satisfactory, and, by generating and fitting many sets of data, have been able to establish some approximate connection formulas between circuit parameters and those listed above. Using these results, one should be able to carry through at least an approximate analysis of intrinsic impedance data without the need of using the full model directly.

ANALYSIS AND RESULTS FOR $\rho_p = 0$, $\rho_n = \infty$

The presence of mobile charges of both signs leads one to expect the appearance of Warburg (diffusion) effects [1,9–13]. The Randles circuit of Fig. 1a is often suggested for such situations when a supporting electrolyte is present [12,13]. Here R_{s0} is the solution (bulk) resistance, C_{dl} the double layer capacitance, R_{CT} a reaction or charge-transfer resistance, and W the Warburg impedance. We need, in general, to add the geometrical capacitance of the cell, C_1 , to this circuit and to replace the non-physical infinite-length Warburg impedance by an impedance Z_D which appears where diffusion occurs over a finite length (finite transmission line) [9,11]. We then obtain the circuit of Fig. 1d with $R_{s0} \rightarrow R_1$, $C_{dl} \rightarrow C_2$, $R_{CT} \rightarrow R_2$, and $W \rightarrow Z_D$.

We shall attempt to apply this circuit, derived for the supported situation, to the intrinsic, unsupported situation. Although a Maxwell or Voigt type of connection of the elements of the circuit might be considered rather than the present ladder network connection [14], it has been shown [11,15] that the latter is generally

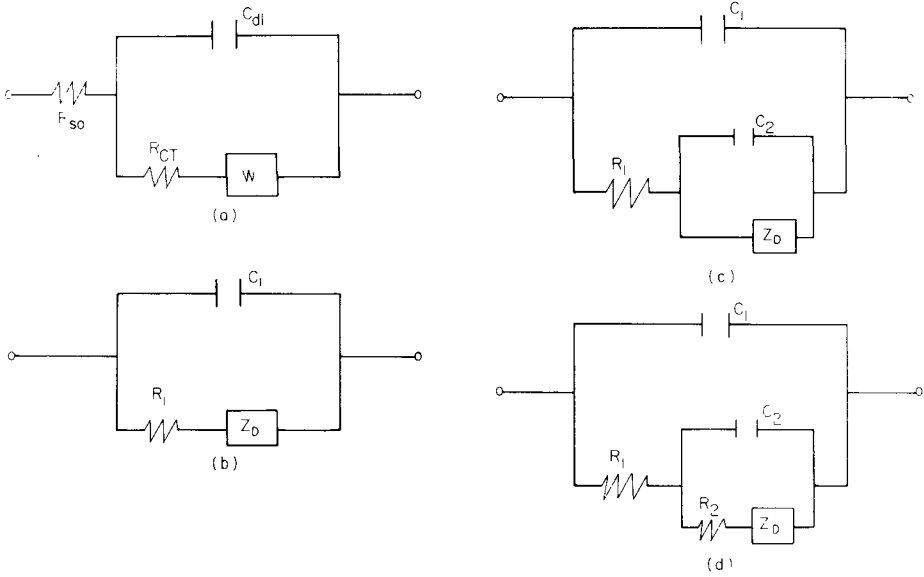


Fig. 1. Possible fitting circuits.

preferable, at least in the unsupported situation. Expression for R_1 and C_1 have already been given. We do not initially have adequate expressions for R_{2N} and C_{2N} in the present case. An approximate analysis of the exact solution with ($\rho_p = 0$ and $\rho_n = \infty$) yielded, however, for the fully dissociated case [1], $R_{2N} = 0$, as expected with an infinite reaction rate, and C_{2N} near the ordinary normalized double layer capacitance expression, $r - 1$, where $r \equiv (M)ctnh(M)$. For Z_{DN} we take the shorted transmission line result [11]

$$Z_{DN} = Z_{DON} (i\Omega H_N^2)^{-1/2} \tanh(i\Omega H_N^2)^{1/2}, \quad (1)$$

where $\Omega H_N^2 \equiv \omega H^2$, so $H_N = H/\tau_D^{1/2}$. In the case of supported diffusion of charge of a single sign, $H \equiv l/\sqrt{D}$, where l is the diffusion length, here the effective electrode separation, and D is the diffusion coefficient of the diffusing quantity. To interpret the results of fitting intrinsic two-mobile data to the circuit of Fig. 1d in terms of microscopic parameters, we need expressions for C_{2N} , R_{2N} , Z_{DON} , and H_N .

In order to simplify our approach as much as possible, we shall generate exact intrinsic data with R_1 and C_1 each taken unity. This leads to no significant loss of generality. Although numerical results for normalized and unnormalized quantities will then be the same, we must maintain the distinction in our formulas in order to allow one to pass properly from normalized to unnormalized expressions. Let $Z_N \equiv Z'_N - iZ''_N$ denote the total normalized impedance and $Y_N \equiv Z_N^{-1} \equiv Y'_N + iY''_N$, the total normalized admittance. Although the full-dissociation data generated seemed to lead to the standard finite-length Warburg shape [9,11,16,17] when Z_N^*

was plotted in the complex plane for given π_m , appreciable shape dependence on π_m was observed when Y_N results were plotted in the complex plane. Here the superscript asterisk indicates complex conjugation. Figure 2 illustrates the behavior obtained for a variety of π_m values. These curves, produced automatically on a plotter, each involved as many as 100 points. The top of the spike of infinite height at $Y'_N = 1$ has been eliminated. Figure 2 shows a surprising variety of shapes with only one of them ($\pi_m = 10^{-2}$) looking at all like the quarter circle one sometimes expects [17] with Warburg processes present. Although the Z_N^* curves increase in size as π_m decreases, they do not change their shape like the Y_N ones do. Clearly as $\pi_m \rightarrow 0$, the Y_N curve approaches a semicircle, a result consistent with the Fig. 1d circuit when $Z_D = \infty$.

We next tried fitting theoretical "data" calculated for a wide range of π_m values to the circuits of Fig. 1b, c, and d using W1 weighting. Results for the standard deviation of overall fit, σ_f , are shown in Fig. 3. All circuits are adequate for $\pi_m \geq 10^{-1}$, but clearly only that of Fig. 1d is appropriate over the entire π_m range investigated. The exact solution [1] shows that in the $\pi_m = 1$ case, where appreciable simplification is possible, the Fig. 1c circuit should be appropriate with $C_{2N} \equiv r - 1$ and $R_{2N} = 0$. In fact, we found it yielded virtually a perfect fit for $\pi_m = 1$. The fitting values of Z_{DON} and H_N obtained with the input values $M = 10^4$, and Λ and ξ both infinite, were 1 and 10^4 , respectively.

Let us continue to restrict attention to the fully dissociated case. Results of much fitting of the Fig. 1d circuit were analyzed, compared with the approximate results of

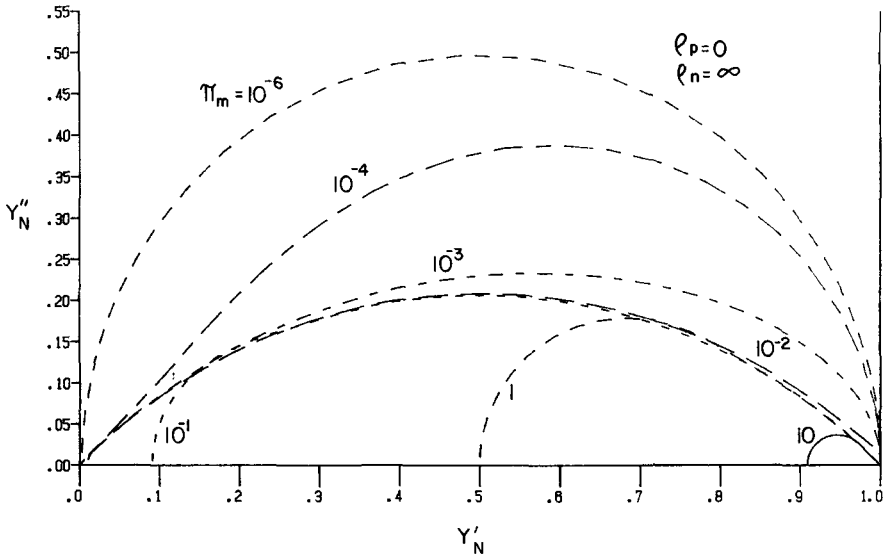


Fig. 2. Admittance plane plots for the normalized admittance, $Y_N \equiv R_1 Y$, for various values of the mobility ratio $\pi_m \equiv \mu_n / \mu_p$.

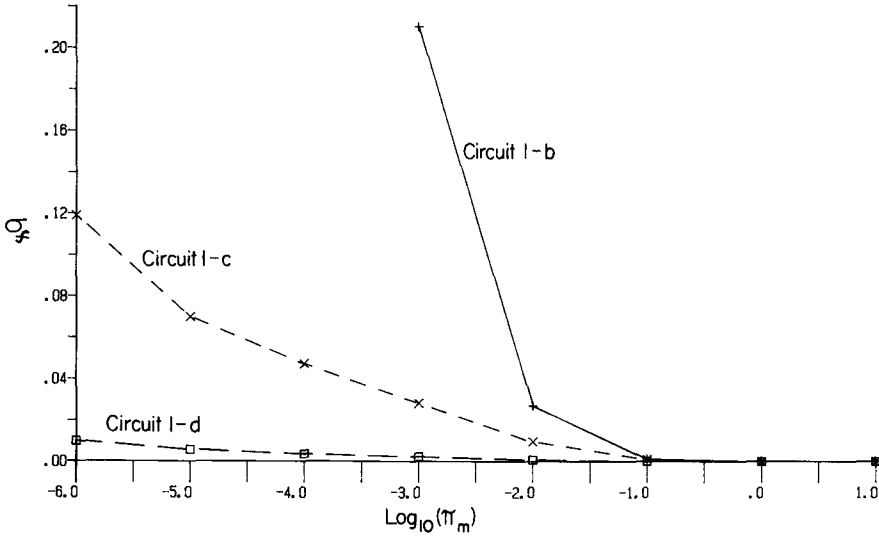


Fig. 3. Overall standard deviation of fit, σ_f , for fitting of the theoretical data to the various circuits of Fig. 1 for a range of π_m values.

the exact solution, and showed that in the $\rho_p = 0$, $\rho_n = \infty$ case, $Z_{\text{DON}} \cong \pi_m^{-1}$ and $H_N \cong (M/2) [\pi_m^{-1} + 2 + \pi_m]^{1/2}$. These particular results agree well with the approximate exact solution results [1]. But the C_{2N} and R_{2N} results did not turn out as expected from the approximate solution. Let us denote R_{2N} as $R_{2N\infty}$ when $\rho_n = \infty$, the present case. We found that $R_{2N\infty}$ was not zero for $\pi_m < 1$ and that C_{2N} was not given by the approximate formula derived in ref. 1 except at $\pi_m = 1$. These results indicate first that the approximations made in simplifying the exact solution were too great, and, more importantly, that an apparent charge transfer resistance can appear when fitting the intrinsic conduction situation even when the electrode reaction rate is infinite for mobile charges of one sign. This implies that possibly serious errors may arise in deriving reaction rates from small-signal impedance results. Since ρ_n will not be infinite in practical cases, we must further investigate such cases and try to derive a method to find ρ_n and k_n in principle no matter what their values. This task is carried out in the next section and shows that there is a practical upper limit to the value of k_n which can be reliably estimated.

The appearance of a $R_{2N} > 0$ in the present ambipolar diffusion situation must be associated with the drag of charges of one sign on those of the other sign when $\pi_m \neq 1$. The resulting R_{2N} is not associated in any way with a charge transfer process when $\rho_n = \infty$ but might be mistaken for a resistance arising from such a process by analogy to the Randles circuit. To clarify the matter, we need an expression for both $R_{2N\infty}$ and for R_{2N} when $\rho_n < \infty$. First, however, consider $\rho_n = \infty$. A few fitting results are shown in Table 1. Here and hereafter we shall always use the Fig. 1d circuit for fitting. In Table 1 σ_f is the standard deviation of the overall fit and

TABLE 1

Some fitting results for $\rho_p = 0$, $\rho_n = \infty$, $\Lambda = \infty$, $\xi = \infty$, and $M = 10^4$. Results are shown in the form N/P , where N is a fitting estimate and P is its standard deviation in %

π_m	Z_{DON}	H_N	C_{2N}	R_{2N}	σ_f
10	0.1	1.739×10^{-4}	$4.46 \times 10^5/0.31$	0	9×10^{-6}
1	1	10^4	9.999×10^4	0	10^{-13}
10^{-2}	99.96/0.01	5.0497/0.01	$6.77 \times 10^3/0.24$	$1.71 \times 10^{-2}/0.53$	6.9×10^{-4}
10^{-6}	$9.97 \times 10^5/0.2$	5.007/0.20	$7.05 \times 10^3/0.20$	$2.09 \times 10^2/1.0$	9.8×10^{-3}

numbers to the right of slashes are the estimated relative per cent standard deviations of the individual parameters. Even the $\pi_m = 10^{-6}$ fit is excellent. Similar results were obtained with other M values.

Although the Z_{DON} and H_N values in the table agree well with the expressions for these quantities given above, those for C_{2N} and R_{2N} do not for $\pi_m < 1$. The C_{2N} dependence is shown in Fig. 4. As $\pi_m \rightarrow 0$, C_{2N} approaches $(r-1)/\sqrt{2}$ or $(r/\sqrt{2})-1$. For $\pi_m > 1$, C_{2N} increases very rapidly. Its dependence in this region is of little interest, however, because its reactance is small there, as is that of the combination $(R_{2N} + Z_D)$ in parallel with it. Thus in this region the bulk parameters R_1 and C_1 dominate. For $\pi_m < 1$, we find that R_{2N} depends on powers of M and $(\pi_m^{-1} - 1)$. By fitting the log of R_{2N} values for many input M and π_m values to an appropriate

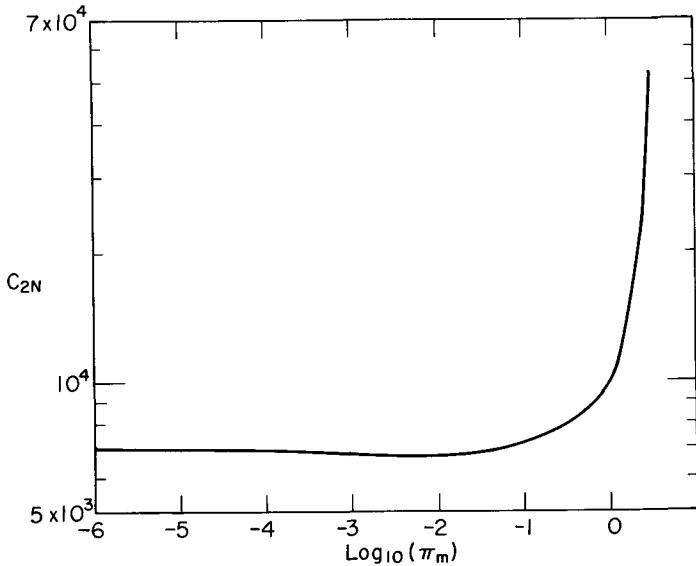


Fig. 4. Dependence of the normalized capacitance, $C_{2N} \equiv C_2/C_1$, on π_m over the π_m range of interest.

function using multiple linear regression, we find

$$R_{2N\infty} \cong 2.815 M^{-1.089} [\pi_m^{-1} - 1]^{1.019} \quad (2)$$

with this result explaining 99.34% of the variation in the data. Nevertheless, this is not a very well-fitting result, and for many purposes, the result obtained from the data by requiring unity exponents,

$$R_{2N\infty} \cong 1.953 M^{-1} [\pi_m^{-1} - 1], \quad (3)$$

will be sufficient. We find that when $\pi_m \ll 1$, $R_{2N\infty}/Z_{\text{DON}} \approx 2/M$. Thus, for sufficiently large M , $R_{2N\infty}$ will be negligible compared to Z_{DON} . But even then, $R_{2N\infty}$ may play a significant role for those $\Omega > 0$ frequency values where $|Z_D| \ll Z_{\text{DON}}$.

Since $R_{2N\infty}$ will be small compared to Z_{DON} for most M values of interest, it is worthwhile to examine how well it can be determined for finite accuracy real data. We simulate this situation by truncating the theoretical data from its original 15 figures to four, three, or two figures. Note that truncation is more severe than rounding and introduces essentially random error. Results are presented in Table 2 where the "remaining figures" column shows the remaining number of figures in the data after any truncation. We see that even the 10% truncation-2 data results are not much degraded from untruncated values and that $R_{2N\infty}$ can still be well determined.

Now although the results of Fig. 2 show that an $R_2 > 0$ is needed to achieve an adequate data fit, Table 1 shows that the fit is still by no means perfect for $\pi_m < 1$, but more serious, the failure of the data to lead to unity exponents in eqn. (2) suggests that the Fig. 1d circuit is still not wholly adequate. We expect a quantity like $R_{2\infty}$ to be intensive, independent of l . But this is only the case for the M^{-1} dependence of eqn. (3). Then one finds that $R_{2\infty}$ may be written in the form

$$R_{2\infty} = 1.953 \left[\frac{\mu_p - \mu_n}{\mu_p + \mu_n} \right] \left[\frac{2L_D}{e\mu_n c_0} \right] \quad (4)$$

entirely l -independent. But the partially extensive behavior of eqn. (2) is not the only

TABLE 2

Fitting results for $\rho_p = 0$, $\rho_n = \infty$, $\Lambda = \infty$, $M = 10^2$ (lines 1-4), $M = 10^4$ (lines 5 and 6), and $\pi_m = 10^{-4}$, showing effects of data truncation

Remaining figures	Z_{DON}	H_N	C_{2N}	R_{2N}	σ_f
15	9760/0.14	4928/0.12	69.5/0.20	211/1.0	9.33×10^{-3}
4	9757/0.14	4929/0.12	69.5/0.20	211/1.0	9.35×10^{-3}
3	9746/0.16	4929/0.12	69.8/0.22	210/1.1	1.01×10^{-2}
2	9656/0.43	4945/0.36	73.0/0.62	202/3.1	2.82×10^{-2}
15	9990/0.05	5.002/0.04	6.98/0.16	1.92/0.78	3.5×10^{-3}
2	9805/0.28	5.034/0.24	7.37/0.87	1.90/4.4	1.60×10^{-2}

TABLE 3

Fitting results for $\rho_p = 0$, $\rho_n = \infty$, $M = 10^2$, and $\pi_m = 10^{-4}$, showing results of Λ and ξ variation

Λ	ξ	Z_{DON}	H_N	C_{2N}	R_{2N}	σ_f
10^2	10^4	$9.76 \times 10^3/0.13$	$4.98 \times 10^3/0.11$	69.7/0.19	207/0.93	8.61×10^{-3}
10^2	10^2	$9.76 \times 10^3/0.14$	$4.98 \times 10^3/0.11$	69.8/0.20	208/0.98	9.08×10^{-3}
10	10^2	$9.80 \times 10^3/0.10$	$5.40 \times 10^3/0.08$	72.6/0.15	185/0.75	6.81×10^{-3}
1	10^2	$9.99 \times 10^3/0.48$	$8.55 \times 10^3/0.33$	85.5/0.81	65.2/5.0	3.38×10^{-2}
10^{-1}	10^2	$1.00 \times 10^4/0.19$	$2.28 \times 10^4/0.15$	70.3/1.6	1.45/22	1.49×10^{-2}
10^{-2}	10^2	$9.71 \times 10^3/0.96$	$7.23 \times 10^4/0.78$	77.9/3.0	6.98/6.2	7.51×10^{-2}

problem. The circuit of Fig. 1d yields the following expression for the total normalized resistance R_{DN} as $\Omega \rightarrow 0$: $R_{\text{DN}} = 1 + R_{2N} + Z_{\text{DO}}$. But the exact solution [1] leads to the exact result

$$R_{\text{DN}} = (1 + \pi_m^{-1})(1 + \rho_n^{-1}) \quad (5)$$

when $\rho_p = 0$. When $\rho_n = \infty$ as well, the two expressions for R_{DN} require that $R_{2N\infty} + Z_{\text{DO}} = \pi_m^{-1}$. But we expect and find that $Z_{\text{DO}} \cong \pi_m^{-1}$. To the degree that this relation is exact, $R_{2N\infty}$ should disappear as $\Omega \rightarrow 0$, even though it plays an important role for non-zero Ω values, particularly those larger than the Ω value which leads to $\text{Max}[IM(Z_D^*)]$, about $2.53 (bM^2)^{-1}$, where $b \equiv (\pi_m + 2 + \pi_m^{-1})/4$. Equation (5) shows that if experimental measurements could be extended to sufficiently low frequencies that $Z_D \rightarrow Z_{\text{DO}} \cong R_{\text{DO}}$, there would be no error in determining the reaction rate constant ρ_n or k_n . But usually, data cannot be obtained at the very low frequencies where zero-frequency results are adequately approximated. Then higher-frequency circuit fitting will generally yield a non-zero R_2 (even when $\rho_n = \infty$), and this resistance will need careful interpretation to avoid errors in reaction rate estimation.

So far we have set the generation–recombination parameters Λ and ξ infinite, appropriate for full dissociation. Comparison of the results presented in Tables 2 and 3 shows that reducing Λ and ξ to 100 makes very little difference in the results. But as Λ continues to decrease and there is less and less dissociation, we see that the overall fit deteriorates, H_N increases and begins to approach Λ^{-1} behavior, and R_{2N} decreases until it is not well defined for Λ appreciably smaller than unity. It thus appears that no R_2 is required in the circuit for strong recombination situations, but we shall not pursue the matter further here and shall take Λ and ξ infinite for the remaining work.

ANALYSIS AND RESULTS FOR $\rho_p = 0$, $\rho_n \leq \infty$

Since the assumption $\rho_n = \infty$ is unduly restrictive, we have carried out numerous fittings with the Fig. 1d circuit of exact intrinsic-model data for which $\rho_n \leq \infty$. Although a proper expression for R_{2N} in the present $\rho_n < \infty$ intrinsic case is not available from theory, earlier work leads to numerous expressions for the charge

transfer resistance in supported [12,13,16] and unsupported [1,15,16] cases when both ρ_p and ρ_n are arbitrary. In the present $\rho_p = 0$, $\rho_n \leq \infty$ situation, the earlier work and eqn. (5) suggest that the contribution to R_{2N} from $\rho_n < \infty$ should be $(1 + \pi_m^{-1})\rho_n^{-1}$. Let us assume that when $\rho_n \leq \infty$, R_{2N} may be written in the form

$$R_{2N} = R_{2N\infty} + R_{2NX} \quad (6)$$

where $R_{2NX} = 0$ for $\rho_n = \infty$. Our task is now to find a good working approximation for R_{2NX} , and thus for R_{2N} in general.

We have obtained R_{2N} results from circuit fitting using a wide variety of M , π_m , and ρ_n values. The corresponding values of $R_{2NX} \equiv (R_{2N} - R_{2N\infty})$ were then calculated using actual fitting $R_{2N\infty}$ values. Again multiple linear regression was employed to find estimates of the parameters in the test function $KM^{-a}(\pi_m^{-1} + 1)^b\rho_n^c$ using the log of R_{2NX} values obtained as above. The result obtained with all parameters free was

$$R_{2NX} \cong 1.197 M^{-0.0322} (\pi_m^{-1} + 1)^{0.9965} \rho_n^{-0.9448} \quad (7)$$

a form that accounted for 99.86% of the variance. But results nearly as good were found with a set to zero and b to 1. Then

$$R_{2NX} \cong 0.927 (\pi_m^{-1} + 1) \rho_n^{-0.942} \quad (8)$$

which still accounted for about 99.81% of the variance. When one sets c to -1 , averaging of the data to obtain K yields

$$R_{2NX} \cong 1.151 (\pi_m^{-1} + 1) \rho_n^{-1} \quad (9)$$

with a relative standard error of fit of about 23%.

It is likely that the reason fitting of R_{2N} results with all exponents free led to slightly non-integral values, as in eqns. (2), (7), and (8), is that even though the Fig. 1d circuit yields good fits of the theoretical data, it is still an approximate representation and induces some systematic error and bias in the fitting results. For most practical purposes, the use of eqns. (3) and (9) will be sufficient for the analysis of experimental data for strongly dissociated systems and will certainly lead to better estimates of k_n than those approaches which neglect $R_{2N\infty}$ entirely. When eqns. (3) and (9) are used in eqn. (6) and $\pi_m \ll 1$, one obtains, for example,

$$R_{2N} \cong \pi_m^{-1} [1.95 M^{-1} + 1.15 \rho_n^{-1}] \quad (10)$$

For obtaining as accurate estimates of K_n and the other system parameters as possible, one should ideally use direct least squares fitting of the data to the intrinsic model without the intermediary of an equivalent circuit.

Now consider how the results of data fitting for a strongly dissociated system can be used to find estimates of microscopic system parameters. First, assume that R_1 , C_1 , R_2 , C_2 , Z_{DO} , and H have been obtained from complex least squares data fitting. If the highest frequency available is too low to yield an adequate estimate of the geometrical capacitance C_1 , it can be calculated when ϵ and l are known. Alternatively, if a value of C_1 is obtained from the fitting, ϵ can be estimated from it. Next,

form R_{2N} , C_{2N} , H_N , and Z_{DON} . We obtain an estimate of π_m directly from $Z_{DON} \cong \pi_m^{-1}$. Then this value may be used in $H_N \cong (M/2)[\pi_m^{-1} + 2 + \pi_m]^{1/2}$ to estimate M . This value of M should usually be preferable to that obtained from $C_{2N} \cong 0.7 [(M)\text{ctnh}(M) - 1]$ which seems to apply for $\pi_m < 0.1$ (see Fig. 4), but the two values should certainly be comparable. Next, $R_{2N\infty}$ may be calculated using eqn. (2) or (3). Then $R_{2NX} \cong R_{2N} - R_{2N\infty}$ may be formed. Finally an estimate of ρ_n may be calculated using eqn. (7), (8), or (9).

Now from the estimate of M found above, one immediately obtains the Debye length L_D . When ϵ is known, it may be used to calculate an estimate of the bulk concentration c_0 . Then using the value of $G_1 \cong R_1^{-1} = (ec_0/l)(1 + \pi_m^{-1})\mu_n$ and the values of c_0 and π_m already found, one obtains estimates of μ_n and μ_p . For a uni-univalent system, $D_i = (kT/e)\mu_i$. Finally, k_n may then be calculated from $k_n \cong 2D_n\rho_n/l$. Thus assuming that l and the electrode area are known, one can calculate from R_1 , C_1 , R_2 , C_2 , Z_{DO} and H the full system characterization parameters L_D , ϵ , c_0 , μ_n , μ_p , ρ_n , and k_n .

Although the above method of data analysis should be useful in most cases of interest, particularly those where k_n is not too large, the accuracy of its k_n estimate necessarily degrades as k_n increases. There is therefore a practical limit to the size of k_n or ρ_n which can be reliably estimated by the present approach, just as there is for other methods of determining k_n . The problem arises from the subtraction $R_{2NX} = R_{2N} - R_{2N\infty}$, where estimates of both members on the right will be uncertain and they approach each other as $k_n \rightarrow \infty$. Let us make the reasonably conservative assumption that the minimum meaningful estimate of this difference, using good but not perfect data, is of the order of $0.5 R_{2N\infty}$. Then the limiting relation $R_{2NX} \cong 0.5 R_{2N\infty}$, yields, using the approximate results of eqns. (3) and (9), the following estimate of the maximum meaningful ρ_n :

$$\rho_{n\max} \cong M(\pi_m^{-1} + 1)/(\pi_m^{-1} - 1) \quad (11)$$

which may usually be adequately approximated as $\rho_{n\max} \cong M$. In turn this result leads to

$$k_{n\max} \cong D_n/L_D. \quad (12)$$

For a D_n of 10^{-6} cm²/s and a L_D of 10^{-5} cm, $k_{n\max}$ is then about 0.1 cm/s.

Finally, it is of interest to examine what sort of error would be made in the estimate of k_n if it were actually very large but this fact was not recognized and R_2 was believed to be R_{2X} , arising from a non-infinite reaction rate, rather than the proper $R_{2\infty}$. This would be the situation mentioned at the beginning of this work where the appearance of $R_2 = R_{2\infty}$ from fitting when ρ_n is actually ∞ is not taken into account. Let us use the approximate result, from Eq. (9), $R_{2NX} \cong (1 + \pi_m^{-1})\rho_n^{-1}$. Then the above misinterpretation amounts to setting $R_{2X} = R_2 = R_{2\infty}$. From this equation, we immediately obtain

$$k_n \cong \frac{2D_n\rho_n}{l} = \frac{2D_n}{l} \frac{(1 + \pi_m^{-1})}{R_{2N}} = 2kT/e^2c_0R_2 = (16\pi/\epsilon)(L_D^2/R_2) \quad (13)$$

For example, if $\epsilon = 5$, $L_D = 10^{-5}$ cm, and $R_2 = 100 \Omega$, one would erroneously obtain $k_n \cong 10^{-11}$ cm/s. Since reaction rates generally fall in the range $10^{-17} \leq k \leq 0.1$, this is a relatively slow rate, far different from the value $k_n \geq 0.1$ one should have obtained with the proper analysis.

ACKNOWLEDGEMENTS

We appreciate the helpful comments of Dr. S.W. Kenkel. This work was supported in part by the University of North Carolina Research Council, the Johnson's Wax Fund, and the U.S. Army Research Office. We are most grateful for this support.

REFERENCES

- 1 J.R. Macdonald and D.R. Franceschetti, *J. Chem. Phys.*, 68 (1978) 1614.
- 2 J.R. Macdonald, D.R. Franceschetti and R. Meudre, *J. Phys. C*, 10 (1977) 1459.
- 3 H.J. Queisser, H.C. Casey, Jr. and W. van Roessbroeck, *Phys. Rev. Lett.*, 26 (1971) 551.
- 4 J.R. Macdonald and J.A. Garber, *J. Electrochem. Soc.*, 124 (1977) 1022.
- 5 J.R. Macdonald, J. Schoonman and A.P. Lehen, *J. Electroanal. Chem.*, 131 (1982) 77.
- 6 Y.-T. Tsai and D.H. Whitmore, *Solid State Ionics*, 7 (1982) 129.
- 7 D.R. Franceschetti, J. Schoonman and J.R. Macdonald, *Solid State Ionics*, 5 (1981) 617.
- 8 J.R. Macdonald, A. Hooper and A.P. Lehen, *Solid State Ionics*, 6 (1982) 65.
- 9 J.R. Macdonald, *J. Electroanal. Chem.*, 32 (1971) 317.
- 10 J.R. Macdonald, *J. Electroanal. Chem.*, 53 (1974) 1.
- 11 D.R. Franceschetti and J.R. Macdonald, *J. Electroanal. Chem.*, 101 (1979) 307.
- 12 J.E.B. Randles, *Discuss. Faraday Soc.* 1 (1947) 11.
- 13 R.D. Armstrong, M.F. Bell and A.A. Metcalfe in H.R. Thirsk (Senior Reporter), *Electrochemistry, Specialist Periodical Report*, Vol. 6, The Chemical Society, London, 1978, p. 98.
- 14 J.R. Macdonald in M. Kleitz and J. Dupuy, (Eds.), *Electrode Processes in Solid State Ionics*, Reidel, Dordrecht, 1976, pp. 149-180.
- 15 D.R. Franceschetti and J.R. Macdonald, *J. Electroanal. Chem.*, 82 (1977) 271.
- 16 J.R. Macdonald, *J. Chem. Phys.*, 61 (1974) 3977.
- 17 J.R. Macdonald in G.D. Mahan and W.L. Roth (Eds.), *Superionic Conductors*, Plenum Press, New York, 1976, pp. 81-97.